Au^{7+} Ion Irradiation Induced Phase Transitions and Morphological Modifications in SnO_2 Thin Films

V. KONDKAR, D. RUKADE

Department of Physics, University of Mumbai, Kalina, Santacruz, Mumbai 400098, India.
Corresponding author: vidya.kondkar@gmail.com

Abstract

Amorphous SnO_2 thin films deposited by thermal evaporation on fused silica are irradiated by Au^{7+} ions with energy 75 MeV at different fluences. Au^{7+} ion irradiation with varied fluences induces the phase transition from amorphous to nanocrystalline phase of SnO_2. Pure orthorhombic to mixed phase transition and increase in nanocrystallite size is noted with the increase in ion fluence. Red shift in the energy band gap from 3.96 eV to 3.65 eV is attributed to increase in the crystallite size on irradiation. Surface morphology studies indicate increase in grain size and grain agglomeration on irradiation. Phase and morphology of irradiated SnO_2 thin films strongly depend on ion fluence.

Keywords: SHI irradiation, Grain agglomeration, nanocrystalline SnO_2, phase transition

Introduction

Nanocrystalline SnO_2 thin films are extensively used in dye-sensitized solar cells, TFTs and gas sensing devices due to improved electrical and gas sensing properties and short response time [1-4]. SnO_2 is a wide band gap semiconductor and typically exists in two crystallographic forms; rutile (tetragonal) and orthorhombic. In the bulk form, rutile is the most stable phase whereas orthorhombic phase is observed only at high pressures and temperatures [5-7]. Several research groups have reported pure as well as mixed phase nanocrystalline SnO_2 thin films using various thin film deposition techniques such as pulsed laser deposition, chemical vapour deposition, RF sputtering and spin coating [6-13]. In most of these techniques, further thermal processing is required for crystalline phase formation. Thermal processing of thin films often leads to wide size distribution that considerably affects device efficiency [4, 14-16]. Swift heavy ion irradiation is widely used technique for modification of thin film properties. Modifications induced in thin film target by SHI irradiation depend on the thin film properties and ion beam parameters such as ion species (mass and charge state), ion energy and ion fluence [17]. Ion beam parameters provide precise control on induced modifications through interaction of ions with target material [18-19]. Thus, SHI irradiation technique proves to be an effective tool for synthesis of thin films with desirable properties. In the present study, synthesis of nanocrystalline SnO_2 thin films by Au^{7+} ion irradiation is reported. Effect of increase in ion fluence on structure and morphology of SnO_2 thin films is discussed.

Experimental

Amorphous SnO_2 thin films of 100 nm thickness are deposited on fused silica substrates using thermal evaporation technique. Commercially available 99.9% pure rutile SnO_2 powder is used for evaporation. These films are irradiated uniformly at room temperature by 75 MeV Au^{7+} ions under high vacuum using 15 UD Pelletron Accelerator at Inter University Accelerator center, New Delhi, India. The

irradiation is carried out at three different fluences namely 1×10^{11} ions/cm^2, 1×10^{12} ions/cm^2 and 1×10^{13} ions/cm^2. The range of Au^{7+} ions in SnO_2 is 6.70 μm as calculated from SRIM 2008.04 [20]. Thus the irradiating ions transfer their energy to the target thin film throughout its thickness and come to rest in the substrate.

Crystalline phase formed after irradiation is identified by glancing angle X-ray Diffraction (GAXRD) using Rigaku Ultima-IV X-Ray Diffractometer and Raman spectroscopy by Renishaw In-Via Raman microscope. Optical studies are carried out using absorption measurement with UV-Vis double-beam spectrophotometer CARY 5000. Surface morphology of the as-deposited and irradiated films is studied using FESEM. A focused electron beam of 5 kV is used to capture the FESEM images.

Results and Discussion

GAXRD Study

Irradiation induced phase and size of the crystallites is determined using GAXRD pattern. Fig. 1 shows GAXRD patterns obtained for as-deposited and irradiated SnO_2 thin films. GAXRD pattern of as-deposited film indicates amorphous nature of the film. GAXRD patterns of the irradiated films show several diffraction peaks corresponding to polycrystalline nature of the films and are in accordance with JCPDS data obtained using PCPDFWIN program. Films irradiated with ion fluences 1×10^{11} ions/cm^2 and 1×10^{12} ions/cm^2 show peaks corresponding to pure orthorhombic phase of SnO_2 (JCPDS, Card No. 78-1063 and 29-1484). A mixed (orthorhombic and tetragonal (T)) phase of SnO_2 is observed for the film irradiated at highest ion fluence (JCPDS, Card No. 78-1063 and Card No. 03-1116). Irradiation induced phase transition shows strong dependence on irradiation fluence.

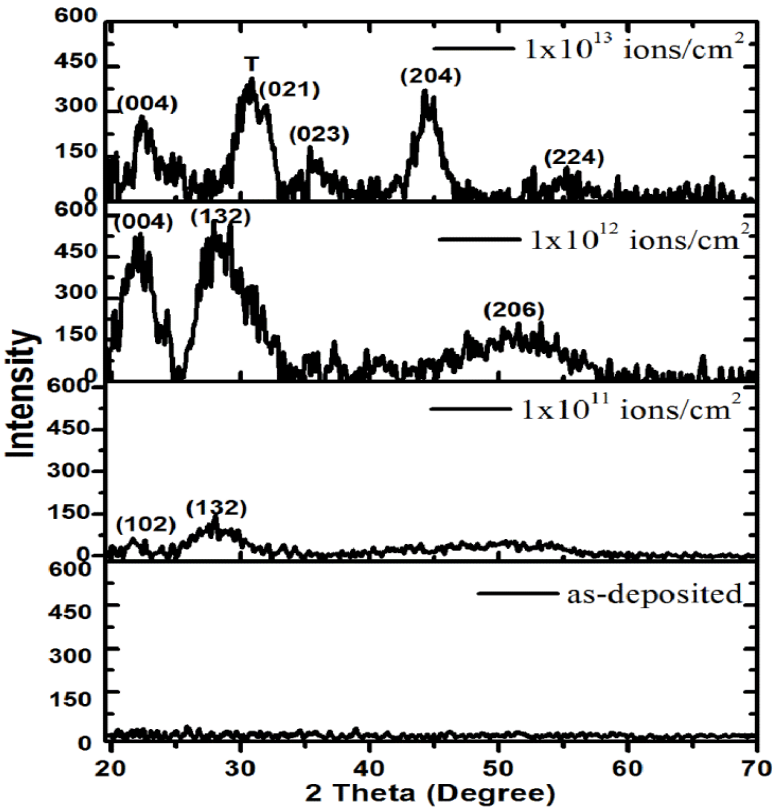

Fig. 1 GAXRD patterns of as-deposited and irradiated SnO_2 thin films.

During SHI irradiation, irradiating ions will transfer huge amount of kinetic energy to the target electrons. If this electronic energy loss (S_e) exceeds threshold value (S_{eth}), dense electronic excitations give rise to cylindrical latent tracks of few nanometres dimensions. Melting of the target material along tracks takes place due to heat dissipation. Further rapid quenching of the melt occurs during heat transfer to much cooler surrounding. If quenching process slows down, atomic motions triggered result in recrystallization of the melt. As the recrystallization process is restricted to the track dimension nanophases formation is expected [17-21]. For 75 MeV Au^{7+} ions in SnO_2 thin films, S_e calculated using SRIM-2008.04 is 19.72 keV/nm. The value of latent track radius (R_e) calculated using Szenes model [22] is 6.57 nm. Hence, formation of nanocrystalline phases with their dimension restricted to 6.57 nm is expected. The average crystallite size determined from FWHM of the XRD peaks using Debye-Scherrer formula is 2 nm, 3 nm and 5 nm for the films irradiated with ion fluence 1×10^{11} ions/cm^2, 1×10^{12} ions/cm^2 and 1×10^{13} ions/cm^2 respectively.

Increase in intensity of the peaks with increase in the ion fluence indicates irradiation enhanced crystallization of the films. Enhanced crystallization in irradiated films occurs due to energy deposition by irradiating ion. Energy density deposited (P) by ion to the target can be calculated using the equation [23],

$$P = S_e / (\pi R_e^2) \quad (1)$$

The value of energy density deposited per ion in our case is 0.145 keV/nm^3. The total amount of energy deposited by ions to the system increases with increase in the ion fluence. At higher fluences, high energy deposition increases crystallization of SnO_2 thin films.

Raman Spectroscopy Study

The Raman spectra obtained by excitation with a 514.5 nm argon laser for as-deposited and irradiated SnO_2 films are shown in Fig. 2. Raman spectrum obtained for the as-deposited film shows very weak intensity peaks near 123 cm^{-1} and 778 cm^{-1} corresponding to B_{1g} and B_{2g} vibrational modes of SnO_2 [24]. These modes are observed with increased intensity in the irradiated films due to crystalline phase formation [25].

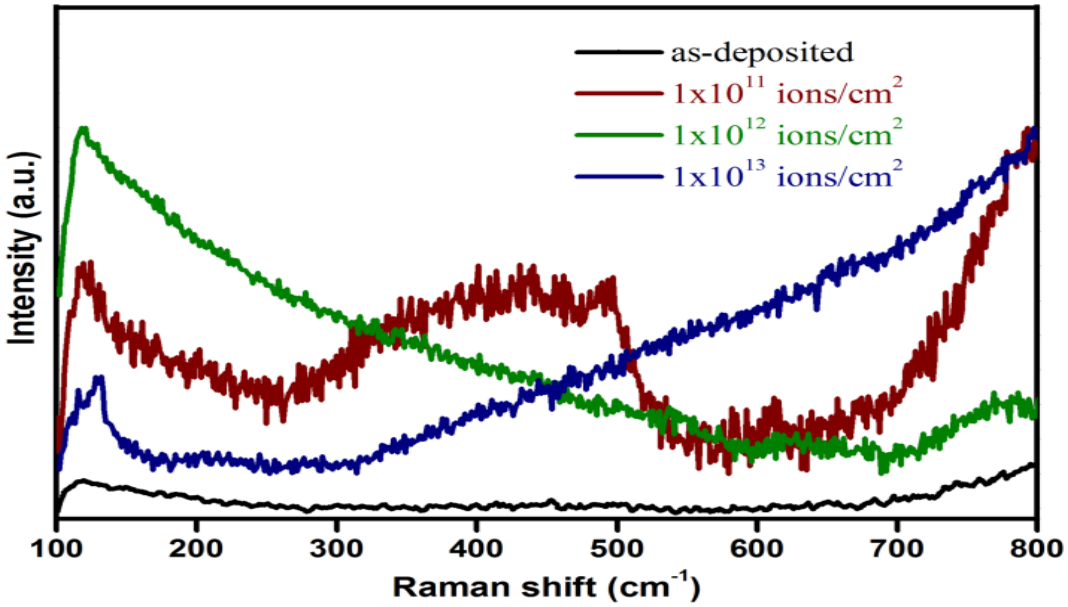

Fig. 2 Raman spectra for SnO_2 thin films.

In case of the film irradiated with ion fluence 1×10^{11} ions/cm^2, a broad peak observed from 300 cm^{-1} to 550 cm^{-1} indicates the presence of A_{2g} and $A_{2u}(TO)$ mode at 425 cm^{-1} and 476 cm^{-1} respectively [26, 27]. This unusual band broadening can be attributed to weak nanocrystalline phase formation and various defects introduced by irradiating ion beam at this fluence [25, 28-29]. Band broadening disappears at higher ion fluences. Increase in crystallinity of the films with increase in the ion fluence is supported by Raman spectra where vibrational modes show improved intensity.

UV-Vis Spectroscopy

Optical energy band gap is measured using UV-Vis absorption spectroscopy. Fig. 3 (a) and 3 (b) show energy band gap calculated for as-deposited and irradiated films using Tauc's plot of $(\alpha h\nu)^2$ versus photon energy hν (eV) where α is absorption coefficient, h is planks constant and ν is frequency of light. The optical band gap (E_g) is determined by extrapolating linear portion of hν at α=0 [30].

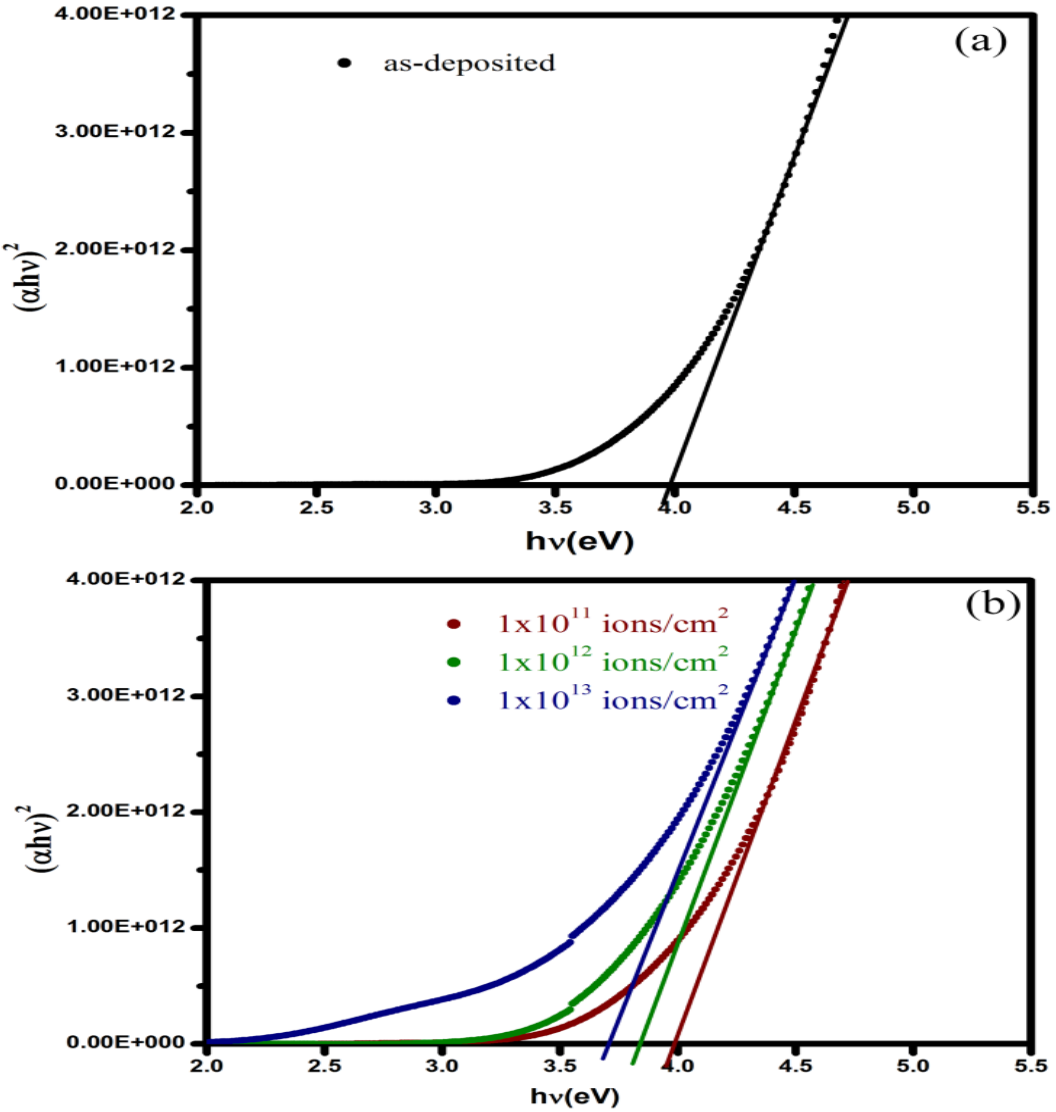

Fig. 3 Plot of $(\alpha h\nu)^2$ versus hν for (a) as-deposited film and (b) irradiated SnO_2 thin films.

The band gap value for the as-deposited film is 3.96 eV. For the film irradiated at fluence 1×10^{11} ions/cm^2 no substantial shift in the band gap is observed. Energy band gap decreases to 3.82 eV and 3.65 eV for ion fluences 1×10^{12} ions/cm^2 and 1×10^{13} ions/cm^2 respectively. This decrease in the band gap is attributed to irradiation induced increase in crystallization evident from GAXRD studies. The value of band gap reported for orthorhombic phase is more than that for tetragonal phase of SnO_2 [6, 11]. Here reduction in the band gap at highest fluence also indicates stoichiometric deviation in SnO_2 thin films [30]. Au^{7+} ion irradiation induced crystallization and phatransition alters the band gap of SnO_2 thin films.

FESEM Study

Variation in surface morphology of the films with ion fluence is studied using FESEM images. Fig. 4(a) shows FESEM image of the as-deposited film. Fig. 4 (b-d) show FESEM images of 75 MeV Au^{7+} ion beam irradiated films at fluences 1×10^{11} ions/cm^2, 1×10^{12} ions/cm^2 and 1×10^{13} ions/cm^2 respectively. The as-deposited film shows spherical grains at film surface. At ion fluence 1×10^{11} ions/cm^2 formation of larger grains is observed. With increase in the ion fluence, grain agglomeration results in formation of nanoclusters. It is also observed that the size of these nanoclusters increases with increase in the ion fluence.

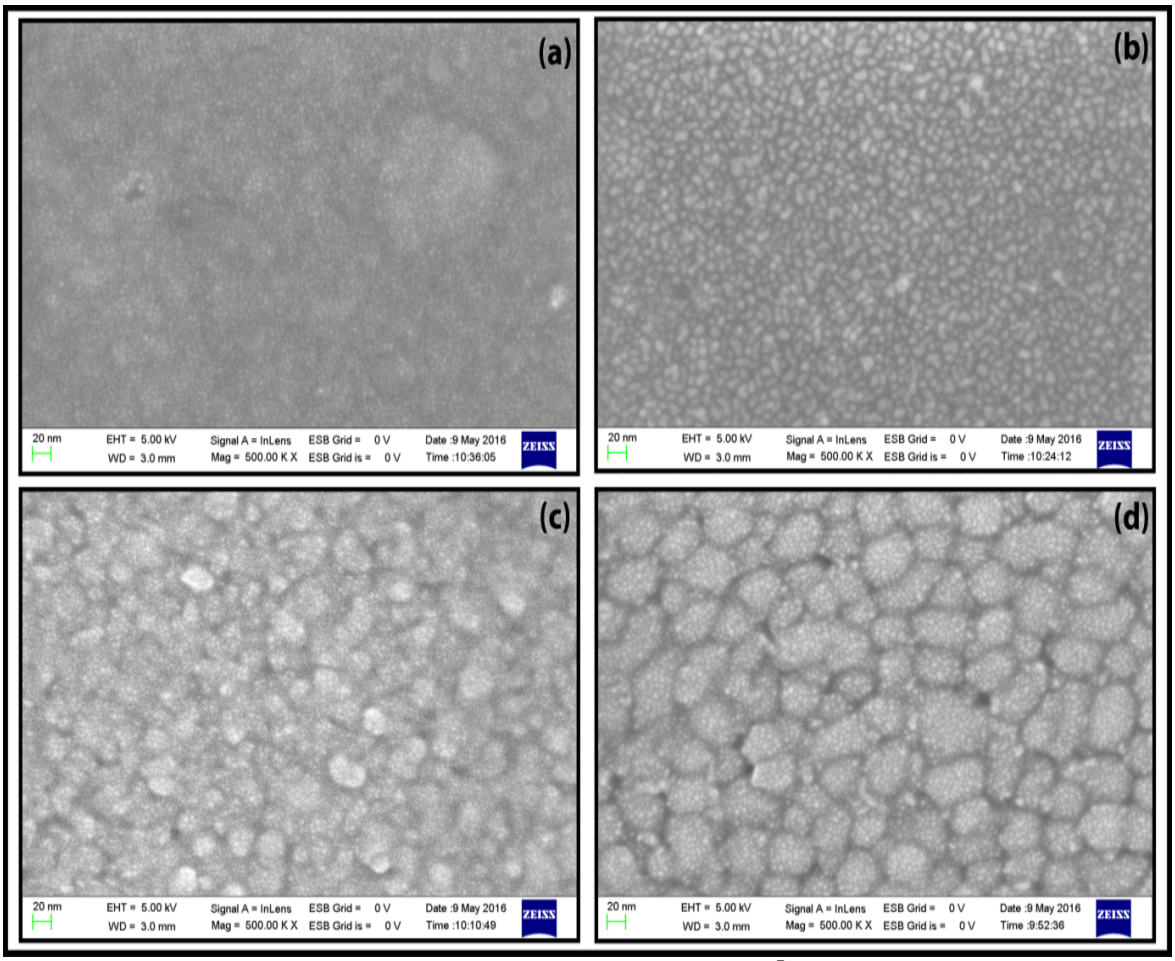

Fig. 4 FESEM images of (a) as deposited SnO_2 thin film and Au^{7+} ion beam irradiated SnO_2 thin films at fluence (b) 1×10^{11} ion/cm^2 (c) 1×10^{12} ions/cm^2 (d) 1×10^{13} ion/cm^2.

Grain size distribution for all the films is studied using histogram plots shown in Fig. 5(a-d). The as-deposited film shows maximum grains in the size range 3-6 nm. For the film irradiated with ion fluence 1×10^{11} ions/cm^2, grain size increases to the range of 6-14 nm. Further increase in the ion fluence leads to nanocluster formation. Insets for Fig. 5 (c) and (d) show size distribution of the nanoclusters observed for the films irradiated at fluence 1×10^{12} ions/cm^2 and 1×10^{13} ions/cm^2 respectively. No such nanoclusters are observed for the film irradiated at ion fluence 1×10^{11} ions/cm^2. For the film irradiated at fluence 1×10^{12} ions/cm^2, nanoclusters with the average size of 20-25 nm are observed. At the highest fluence, bigger nanoclusters grow further up to ~70 nm. For both the fluences, nanoclusters are made of evenly distributed smaller grains of ~4 nm.

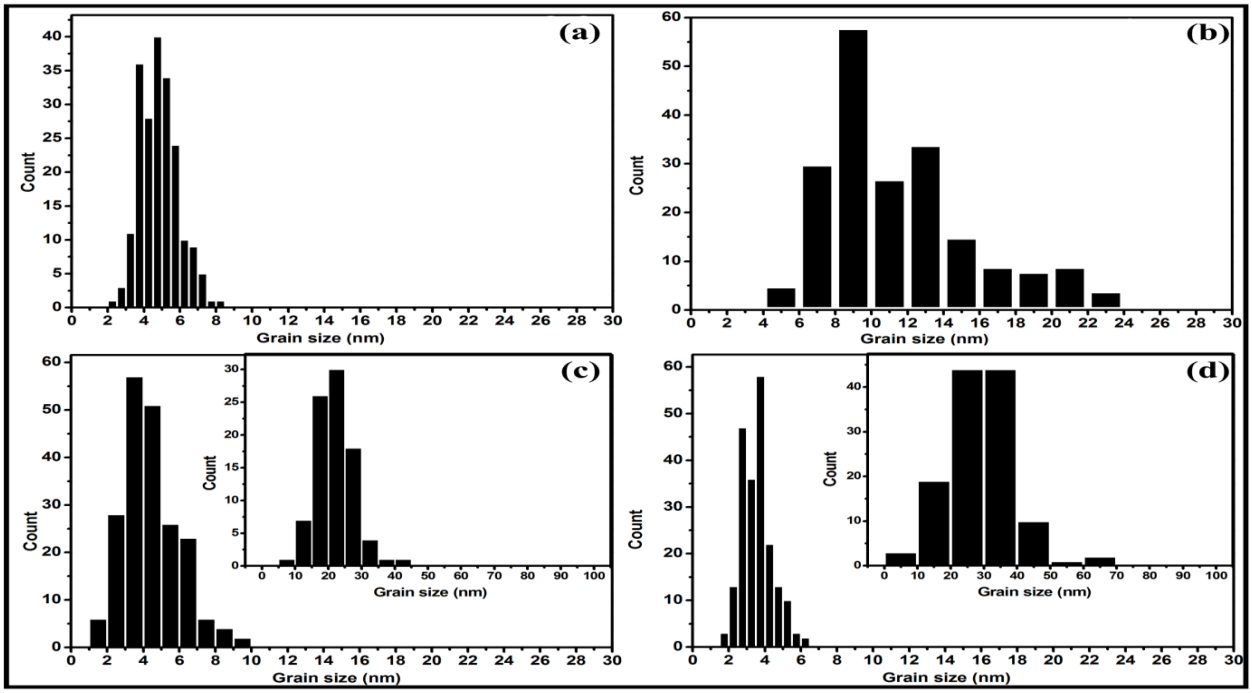

Fig. 5 Grain size distribution of (a) as-deposited SnO_2 thin film and Au^{7+} ion beam irradiated SnO_2 thin films at fluence (b) 1×10^{11} ion/cm^2 (c) 1×10^{12} ions/cm^2 (d) 1×10^{13} ion/cm^2.

FESEM studies indicate ion beam induced grain growth and grain agglomeration with increase in the ion fluence. Equation 1 shows total amount of energy deposited to the system increases with increase in the ion fluence. This releases greater heat which tends to increase system temperature. At higher temperatures, grain boundary pinning prevents individual grain growth and nanocluster formation due to grain agglomeration is observed [31]. Increase in grain agglomeration at highest fluence results in bigger nanocluster formation.

Conclusion

Au^{7+} ion irradiation induced structural and morphological modifications in amorphous SnO_2 thin films have been studied. Irradiation at lower fluences induces pure orthorhombic phase. Mixed phase of orthorhombic and tetragonal SnO_2 is reported at the highest fluence. Red shift of the band gap is attributed to irradiation induced crystallization. FESEM study reveal irradiation induced grain size increase and nanocluster formation with increase in the ion fluence. Energy deposition by irradiating Au^{7+} ions control phase transition and morphological modifications in SnO_2 thin films.

Acknowledgments

Authors are grateful to Dr. Kanjilal IUAC, New Delhi for the ion beam facility. Thanks are due to Dr. Asokan Kandasami for the help rendered during irradiation experiment at IUAC, New Delhi. V. K. Author is thankful to Mr. Ajit Mahadkar, TIFR for thin film deposition. We would also like to thank INUP, CEN, IIT Bombay for FESEM facility.

References

[1] Y. El-Etre and S. M. Reda, "Applied Surface Science Characterization of nanocrystalline SnO_2 thin film fabricated by electrodeposition method for dye-sensitized solar cell application," Appl. Surf. Sci., vol. 256, pp. 6601–6606, 2010. doi:10.1016/j.apsusc.2010.04.055

[2] K. Jo, S. Moon, and W. Cho, "Fabrication of high-performance ultra-thin-body SnO_2 thin-film transistors using microwave-irradiation post-deposition annealing," Appl. Phys. Lett., vol. 106, p. 43501, 2015. doi:10.1063/1.4906863

[3] E. N. Dattoli, Q. Wan, W. Guo, Y. Chen, X. Pan, and W. Lu, "Fully Transparent Thin-Film Transistor Devices Based on SnO_2 Nanowires," Nano Lett., vol. 7, no. 8, pp. 2463–2469, 2007. doi:10.1021/nl0712217

[4] S. Rani, S. C. Roy, N. K. Puri, M. C. Bhatnagar, and D. Kanjilal, "Enhancement of Ammonia Sensitivity in Swift Heavy Ion Irradiated Nanocrystalline SnO_2 Thin Films," J. Nanomater., vol. 2008, p. 395490, 2008. doi:10.1155/2008/395490.

[5] M. Batzill and U. Diebold, "The surface and materials science of tin oxide," Prog. Surf. Sci., vol. 79, pp. 47–154, 2005. doi:10.1016/j.progsurf.2005.09.002

[6] Z. Chen, J. K. L. Lai, and C. H. Shek, "Facile strategy and mechanism for orthorhombic SnO_2 thin films," Appl. Phys. Lett., vol. 89, p. 231902, 2006. doi:10.1063/1.2399352

[7] Z. W. Chen, C. M. L. Wu, C. H. Shek, J. K. L. Lai, Z. Jiao, and M. H. Wu, "Pulsed Laser Ablation for Tin Dioxide: Nucleation , Growth , and Microstructures Pulsed Laser Ablation for Tin Dioxide: Nucleation , Growth , and Microstructures," Crit. Rev. Solid State Mater. Sci., vol. 33, pp. 197–209, 2008. doi:10.1080/10408430802415006

[8] J. E. Dominguez et al., "Epitaxial SnO_2 thin films grown on (1012) sapphire by femtosecond pulsed laser deposition," J. Appl. Phys., vol. 91, no. 3, pp. 1060–1065, 2002. doi:10.1063/1.1426245

[9] F. J. Lamelas and S. A. Reid, "Thin-film synthesis of the orthorhombic phase of SnO_2," Phys. Rev. B, vol. 60, no. 13, pp. 9347–9352, 1999. doi:10.1103/physrevb.60.9347

[10] P. Rajaram, Y. C. Goswami, S. Rajagopalan, and V. K. Gupta, "Optical and structural properties of SnO_2 films grown by a low-cost CVD technique," Mater. Lett., vol. 54, pp. 158–163, 2002. doi: 10.1016/s0167-577x(01)00555-9

[11] L. Kong, J. Ma, Z. Zhu, C. Luan, X. Yu, and Q. Yu, "Synthesis of orthorhombic structure epitaxial tin oxide fim," Mater. Lett., vol. 64, pp. 1350–1353, 2010. doi:10.1016/j.matlet.2010.03.058.

[12] S. Hamzaoui and M. Adnane, "Effects of temperature and r . f . power sputtering on electrical and optical properties of SnO_2," Appl. Energy, vol. 65, pp. 19–28, 2000. doi:10.1016/s0306-2619(99)00045-8.

[13] L. M. Cukrov, P. G. Mccormick, K. Galatsis, and W. Wlodarski, "Gas sensing properties of nanosized tin oxide synthesised by mechanochemical processing," Sensors and actuators, vol. 77, pp. 491–495, 2001. doi:10.1016/s0925-4005(01)00751-1.

[14] M. Thakurdesai, A. Mahadkar, D. Kanjilal, and V. Bhattacharyya, "Nanocrystallisation of TiO_2 induced by dense electronic excitation," Vacuum, vol. 82, pp. 639–644, 2008. doi:10.1016/j.vacuum.2007.10.002

[15] N. Yamazoe, "New approaches for improving semiconductor gas sensors," Sensors and actuators, vol. 5, pp. 7–19, 1991. doi:10.1016/0925-4005(91)80213-4

[16] Wang, L. Yin, L. Zhang, D. Xiang, and R. Gao, "Metal Oxide Gas Sensors: Sensitivity and Influencing Factors," Sensors, vol. 10, pp. 2088–2106, 2010. doi:10.3390/s100302088.

[17] T. Mohanty, S. Dhounsi, P. Kumar, A. Tripathi, and D. Kanjilal, "Surface & Coatings Technology 250 keV Ar^{2+} ion beam induced grain growth in tin oxide thin films," Surf. Coat. Technol., vol. 203, pp. 2410–2414, 2009. doi:10.1016/j.surfcoat.2009.02.108

[18] R. S. Chauhan et al., "SHI irradiation induced amorphization of nanocrystalline tin oxide thin film at low temperature," Adv. Mater. Lett., vol. 5, no. 11, pp. 666–670, 2014. doi:10.5185/amlett.2014.nib501

[19] S. Dhara, "Formation, Dynamics, and Characterization of Nanostructures by Ion Beam Irradiation," Crit. Rev. Solid State Mater. Sci., vol. 32, pp. 1–50, 2007. doi:10.1080/1040843060118762

[20] F. Ziegler, J. P. Biersack, and U. Littmark, The Stopping and Range of Ions in Solids. New York: Pergamon, 1985.

[21] M. Thakurdesai, T. Mohanty, J. John, T. K. Gundu Rao, Pratap Raychaudhuri, V. Bhattacharyya, and D. Kanjilal, "Synthesis of Nanodimensional TiO_2 Thin Films," J. Nanosci. Nanotechnol., vol. 8, pp. 1–7, 2008. doi:10.1166/jnn.2008.032.

[22] G. Szenes, Z. E. Horvath, B. Pecz, F. Paszti, and L. Toth, "Tracks induced by swift heavy ions in semiconductors," Phys. Rev. B, vol. 65, p. 45206, 2002. doi:10.1103/physrevb.65.045206.

[23] Dunlop, G. Jaskierowicz, J. Jensen, and S. Della-Negra, "Track separation due to dissociation of MeV C_{60} inside a solid," Nucl. Instrum. Methods Phy. Res. B, vol. 132, pp. 93–108, 1997. doi:10.1016/s0168-583x(97)00390-x

[24] K. Mcguire, Z. W. Pan, Z. L. Wang, D. Milkie, J. Menéndez, and A. M. Rao, "Raman Studies of Semiconducting Oxide Nanobelts," J. Nanosci. Nanotechnol., vol. 2, pp. 1–4, 2002. doi:10.1166/jnn.2002.129

[25] P. K. Kuiri, H. P. Lenka, J. Ghatak, G. Sahu, B. Joseph, and D. P. Mahapatra, "Formation and growth of SnO_2 nanoparticles in silica glass by Sn implantation and annealing Formation and growth of SnO_2 nanoparticles in silica glass," J. Appl. Phys., vol. 102, p. 24315, 2007. doi:10.1063/1.2761778.

[26] J. Q. Hu, X. L. Ma, N. G. Shang, Z. Y. Xie, N. B. Wong, C. S. Lee, and S. T. Lee, "Large-Scale Rapid Oxidation Synthesis of SnO_2 Nanoribbons," J. Phys. Chem., vol. 106, pp. 3823–3826, 2002. doi:10.1021/jp0125552

[27] A. Sharma, M. Varshney, K. D. Verma, Y. Kumar, and R. Kumar, "Nuclear Instruments and Methods in Physics Research B Structural and surface microstructure evolutions in SnO thin films under ion irradiation," Nucl. Instrum. Methods Phy. Res. B, vol. 308, pp. 15–20, 2013. doi:10.1016/j.nimb.2013.04.054

[28] Dieguez, A. Romano-rodriguez, A. Vila, and J. R. Morante, "The complete Raman spectrum of nanometric SnO_2 particles The complete Raman spectrum of nanometric SnO_2 particles," J. Appl. Phys., vol. 90, no. 3, pp. 1550-1557, 2001. doi:10.1063/1.1385573

[29] S. Das, S. Kar, and S. Chaudhuri, "Optical properties of SnO_2 nanoparticles and nanorods synthesized by solvothermal process Optical properties of SnO_2 nanoparticles and nanorods

synthesized by solvothermal process," J. Appl. Phys., vol. 99, p. 114303, 2006. doi:10.1063/1.2200449.

[30] H. Thakur, K. K. Sharma, R. Kumar, P. Thakur, Y. Kumar, A. P. Singh, S. Gautam, and K. H. Chae, "On the Optical Properties of Ag^{+15} Ion-beam-irradiated TiO_2 and SnO_2 Thin Films," J. Korean Phys. Soc., vol. 61, no. 10, pp. 1609–1614, 2012. doi:10.3938/jkps.61.1609

[31] R. Shugurov, A. V Panin, H. G. Chun, and B. A. Loginov, "Grain Growth and Thermal Stability of Ag Thin Films," Proceedings. The 9th Russian-Korean International Symposium on Science and Technology, (KORUS 2005), pp. 528-531, 2005. doi:10.1109/KORUS.2005.1507775. (Conference proceedings)